Tropospheric ozone evolution between 1890 and 1990

J.-F. Lamarque, P. Hess, L. Emmons, L. Buja, W. Washington, Claire Granier

Tropospheric ozone evolution between 1890 and 1990

J.-F. Lamarque, P. Hess, and L. Emmons
Atmospheric Chemistry Division, National Center for Atmospheric Research, Boulder, Colorado, USA

L. Buja and W. Washington
Climate and Global Dynamics Division, National Center for Atmospheric Research, Boulder, Colorado, USA

C. Granier[1]
Service d'Aéronomie, Institut Pierre-Simon Laplace, Paris, France

Received 21 October 2004; revised 13 January 2005; accepted 3 February 2005; published 26 April 2005.

[1] In this study, we have performed a set of simulations to detail the evolution of tropospheric ozone from 1890 to 1990. The simulations are compared with available measurements for present-day conditions and earlier. Using our best estimates of ozone precursors emissions (based on the work by van Aardenne et al. (2001)), we have found a tropospheric ozone burden increase of 71 Tg between 1890 and 1990, an increase of ~30%. When no anthropogenic emissions in 1890 are considered, this burden increase reaches 88 Tg. The ozone lifetime is shown to have decreased by ~30%, especially after 1930. It is also shown that the net chemical production in the lower troposphere exceeded that in the free troposphere for the first time in the 1950–1970 period. In addition, the ozone production in this study increased rapidly between 1890 and 1930 and from 1970 to 1990. However, the ozone production efficiency in the troposphere is shown to have decreased during the 20th century, making the troposphere less NO_x limited. Finally, a decrease in the OH burden is estimated to be on the order of 8%, matched by a similar increase in the CO lifetime.

Citation: Lamarque, J.-F., P. Hess, L. Emmons, L. Buja, W. Washington, and C. Granier (2005), Tropospheric ozone evolution between 1890 and 1990, *J. Geophys. Res.*, *110*, D08304, doi:10.1029/2004JD005537.

1. Introduction

[2] The distribution of ozone in the troposphere and lower stratosphere is an important component to the atmospheric radiative forcing [*Lacis et al.*, 1990; *Shine and de Forster*, 1999]. The observed ozone increase over the 20th century [*Marenco et al.*, 1994; *Staehelin et al.*, 2001] is estimated to be the third largest increase in direct radiative forcing since the preindustrial period [*Ramaswamy et al.*, 2001]. Numerous modeling studies have highlighted the role of anthropogenic emissions of ozone precursors as the main source for this increase [e.g., *Berntsen et al.*, 1997; *Levy et al.*, 1997; *Roelofs et al.*, 1997; *Brasseur et al.*, 1998; *Stevenson et al.*, 1998; *Wang and Jacob*, 1998; *Mickley et al.*, 1999; *Lelieveld and Dentener*, 2000; *Hauglustaine and Brasseur*, 2001; *Shindell et al.*, 2003; *Wong et al.*, 2004]. In all these studies, the focus has been on contrasting the present-day ozone distribution with the distribution before any significant industrial activity. Consequently, they assumed no anthropogenic emissions and considered the biomass burning emissions to be only a fraction of the present-day estimate (usually 10%).

[3] The motivation for this study comes from the need by climate models for time-varying ozone distributions from the end of the 19th century until the end of the 20th century. For this purpose, we rely on estimates of anthropogenic emissions from *van Aardenne et al.* [2001]. These emissions indicate some significant industrial activity was present in 1890, at least in the Northern Hemisphere. Because most historical emissions of ozone precursors are quite uncertain [*Mickley et al.*, 2001], we will investigate the role of the various sources of tropospheric ozone in shaping its distribution in 1890 and 1990. Therefore we have used a new tagging method that keeps track of the ozone produced in association with a specified source of nitrogen oxides (NO_x = NO + NO_2). This procedure enables the analysis of the role of specific surface NO_x sources to the tropospheric ozone budget. The radiative forcing associated with the simulated ozone distribution will be discussed in another paper (W. J. Collins et al., manuscript in preparation, 2005) and will not appear here.

[4] This paper is organized as follows: in section 2, we describe the global chemistry transport model used for the simulations. The emissions and boundary conditions needed by this model are described in section 3. Then we compare our model results with available observations. The evolution of surface ozone during the 1890 to 1990 period is presented in section 5. Then the sources of surface ozone between 1890 and 1990 are contrasted in section 6. We discuss the evolution of ozone budget terms during the 20th

[1] Also at Cooperative Institute for Research in Environmental Sciences, NOAA, Aeronomy Laboratory, Boulder, Colorado, USA.

0148-0227/05/2004JD005537

century in section 7. Finally the overall results are discussed and conclusions are drawn in section 8.

2. Model Description

[5] The Model for Ozone and Related chemical Tracers version 2 (MOZART-2) chemistry transport model was originally developed at the National Center for Atmospheric Research, the Geophysical Fluid Dynamics Laboratory and the Max-Planck Institute for Meteorology to study tropospheric chemistry. For a complete description of the model and its evaluation, the reader is referred to *Horowitz et al.* [2003] and references therein.

[6] MOZART-2 provides the distribution of 80 chemical constituents (including nonmethane hydrocarbons) between the surface and the stratosphere. In this study, we use the model at a uniform horizontal resolution of $\sim$2.8° in both latitude and longitude. The vertical discretization of the meteorological data (described below) and hence of the model consists of 18 hybrid levels from the ground to $\sim$4 hPa. The evolution of species is calculated with a time step of 20 min. We use meteorological fields provided by the Parallel Climate Model [*Washington et al.*, 2000] valid for the period of interest (available from 1890 to 1990 in increments of 20 years). This simulation considers all the known climate forcings, including greenhouse gases, aerosols and volcanoes. The fields for 2 consecutive years, at each 20-year increment, were saved every 3 hours to ensure a reasonable representation of transport. The model is run for 3 years by repeating the first year as spin-up. The following 2 years are used for analysis.

[7] Because of the relatively coarse vertical resolution of the meteorological data set, we have included the SYNOZ [*McLinden et al.*, 2000] parameterization of stratosphere-troposphere exchange (STE) of ozone, with an annual global average flux of 400 Tg/yr, at the low end of fluxes in global models [*Prather et al.*, 2001]. This low value was chosen as to provide a lower bound on the role of stratospheric ozone in the tropospheric ozone budget, especially under preindustrial conditions. Because the ozone STE is still somewhat dependent on the meteorology of a specific year this parameterization allows for some interannual variability (on the order of 10%) in the STE of ozone (it will be exactly 400 Tg/yr only at steady state).

[8] The tropospheric photolysis rates use a vertical distribution of ozone based on the simulated ozone in the troposphere and on the climatology from *Kiehl et al.* [1999] above. For each simulation, this latter distribution is updated to reflect the changes in the lower stratosphere during the 20th century, affecting only the photolysis rates and not the amount of ozone transported from the stratosphere.

[9] In this study, we have tagged the ozone produced as a result of the hydrocarbon oxidation in association with a specific source of tagged NO_x. To take into account the recycling of NO_x from reservoirs such as PAN, this tagging procedure includes all the nitrogen-containing compounds. This tagged ozone is destroyed at the same rate as the full ozone. If the tagged NO_x takes into account all tropospheric NO_x sources, then the tagged ozone is a very good approximation to the ozone of tropospheric origin. Although there are some minor pathways to create ozone without the presence of NO_x, the accuracy of this tagged ozone has been estimated to be better than 95% on monthly timescales. The accuracy of the system was checked by comparing ozone changes in the lower troposphere with the full ozone and with the tagged schemes (over a period of a few days). In addition, we made use the stratospheric ozone tracer described by *Horowitz et al.* [2003] in our analysis; it is set equal to stratospheric ozone and transported into the troposphere, where it is destroyed at a rate defined by the main pathways of ozone destruction. Because of the assumptions involved in the tropospheric loss rate of the stratospheric ozone tracer, its distribution can be somewhat inaccurate [*Emmons et al.*, 2003]. Therefore, when available (because of the additional computational cost, we have only used the tagged ozone procedure for the 1890 and 1990 cases), we have used the difference between total ozone and the tagged ozone (tagged using all tropospheric NO_x sources) to diagnose the stratospheric portion of the ozone concentration. However, the overall conclusions are unaffected by the choice of measure for stratospheric ozone.

Table 1. Time Evolution of the Global Total (Anthropogenic and Natural) Emissions for Selected Species[a]

	CO	NO	C_2H_4	C_2H_6	C_3H_6	C_3H_8	CH_2O	SO_2
1890	419.1	15.3	9.7	3.8	3.7	3.7	1.4	32.4
1900	469.0	16.8	10.1	4.1	3.9	3.8	1.6	33.9
1910	501.4	18.9	10.6	4.7	4.0	4.2	1.8	35.4
1920	534.0	20.6	11.2	5.2	4.2	4.4	2.1	36.9
1930	574.9	22.7	11.7	5.9	4.4	4.9	2.3	38.7
1940	608.6	24.5	12.2	6.4	4.6	5.3	2.5	40.2
1950	653.4	29.3	12.6	6.3	4.7	5.2	2.6	42.9
1960	760.8	38.5	13.7	7.8	5.1	6.9	3.1	49.9
1970	841.9	49.0	15.2	11.0	5.6	11.7	3.7	55.6
1980	914.7	62.7	15.8	14.2	5.9	17.9	3.9	62.7
1990	976.0	73.8	15.4	10.9	6.0	10.2	3.4	69.2

[a]Emissions in Tg (species)/yr.

3. Emissions and Boundary Conditions

[10] The emissions of all chemical species are based on the EDGAR-HYDE 1.4 database [*van Aardenne et al.*, 2001, see http://arch.rivm.nl/env/int/coredata/edgar/edgar-hyde-100y.html]. These gridded global emissions of CO, NO_x and nonmethane hydrocarbons are based on historical activity data and are available every 10 years. These emissions were shown to compare very well to other published estimates available for limited periods and/or regions [*van Aardenne et al.*, 2001]. The global annual totals (anthropogenic and natural sources) used in this study are given in Table 1 for selected species. The seasonal cycle in emissions is taken to be the same as in our estimated present-day emissions; in particular, we assume no seasonality in anthropogenic emissions.

[11] To fit our set of modeled chemical species, we have made the assumption that the 1990 MOZART-2 speciation of the nonmethane hydrocarbon emissions (only the total amount of all nonmethane hydrocarbons emissions is available from EDGAR-HYDE 1.4) was valid for the entire period of study.

[12] Between 1890 and 1990 emissions of NO_x have experienced an almost exponential increase, from about 15 Tg(NO)/yr to $\sim$75 Tg(NO)/yr (Table 1). Similar increases are found for other ozone precursors. In the case of NO_x this growth comes mostly from direct anthropogenic emissions, in addition to soil fertilization and increased

biomass burning. The soil NO_x emissions are taken from *van Aardenne et al.* [2001], which takes increased fertilizer use into account. Aircraft emissions are set to 0 for 1890 through 1930, while the 1940–1980 period used 10%, 20%, 40%, 60%, 80% of present emissions, respectively.

[13] Global estimates of biomass burning emissions are very uncertain, even for present-day conditions where satellite information is available [*van der Werf et al.*, 2003; *Ito and Penner*, 2004; *Tansey et al.*, 2004]. Most studies of preindustrial ozone have assumed a reduction in biomass burning to one tenth of its present-day estimate. However, the forest fire record derived from Greenland ice cores indicates several very large boreal forest fires in the decades around 1900 [*Holdsworth et al.*, 1996; *Savarino and Legrand*, 1998]. This occurrence is also corroborated by the analysis of charcoal data in lake sediments from North America [*Clark*, 1988; *Clark and Robinson*, 1993; *Campbell and Flannigan*, 2000]. We have therefore decided to keep the boreal forest fires emissions at their present-day level.

[14] Over the tropical regions, we follow the EDGAR-HYDE recommendation; that is, it is assumed that half of the present-day savanna fires are of natural origin [*van Aardenne et al.*, 2001]. Therefore, in 1890, we only use half of the present-day emissions from savanna fires. In addition, EDGAR-HYDE assumes that the impact of increasing deforestation in the tropical regions is a consequence of the development of a rural population. Consequently the tropical CO emissions from biomass burning (savanna and forests) in 1890 are ~30% of their 1990 value [see *van Aardenne et al.*, 2001, Table 6]; intermediate periods are characterized by a ramping up from 1890 to 1990 values. Emissions from the combustion of biofuels are included in the anthropogenic emissions of EDGAR-HYDE.

[15] The NO_x production by lightning follows the *Price et al.* [1997] parameterization, as discussed by *Horowitz et al.* [2003]. It is scaled to a specified global annual amount; in our case, we specify this amount to be 5 Tg(N)/yr (as in the work by *Gauss et al.* [2003]) for the 1990 case. The same parameters were then applied to all simulations, in which the NO_x production can therefore respond to climate change. However, no significant variation of this global amount over the simulated period was found (not shown).

[16] The biogenic emissions of isoprene are calculated off line using the algorithms developed by *Guenther et al.* [1995], taking into account the simulated surface temperature and solar flux at the surface valid for each simulated period. This creates an increase of ~40 Tg/yr between 1890 (481 Tg/yr) and 1990 (527 Tg/yr) in the annual global integral of isoprene emissions. Because no land use or land cover change is considered in this exercise, modifications to the biogenic emissions are solely due to a temperature effect (no significant changes in photosynthetically active radiation during the 20th century were found in this study). However, it must be mentioned that this range of increase is not statistically significant as such interannual variability can be found in present-day conditions (as calculated in an independent 10-year calculation, not shown). All the remaining natural emissions are kept at present-day values [see *Horowitz et al.*, 2003].

[17] For each simulation, the surface concentration of methane is set to a fixed value obtained from *Prather et al.* [2001]. The regional and seasonal variations in surface concentration are set by adjusting the observed present-day distribution by the ratio of the total methane emissions (calculated using the anthropogenic emissions of methane from *van Aardenne et al.* [2001] and assuming constant natural emissions) between the considered period (say 1890) and 1990. The H_2 surface concentration is scaled using the same procedure as methane. In addition, since the MOZART-2 model uses a climatological distribution of sulfate aerosols [see *Horowitz et al.*, 2003], this aerosol loading is scaled in each simulation according to the SO_2 emissions from EDGAR-HYDE and assuming constant dimethylsulfide (DMS) emissions.

4. Comparison With Ozone Observations and Discussion

[18] In this section we present the comparison of our modeled ozone distribution with available observations for several periods. In addition, we include a discussion of the quality of the preindustrial record and of several sensitivity experiments in which we have modified the ozone dry deposition and the emission inventories.

4.1. Present-Day Simulation

[19] To evaluate the 1990 simulated ozone distribution, we use the *Logan* [1999] ozonesonde climatology. Results from selected stations (selected to provide a wide latitudinal sampling and a similar distribution to the 1890 stations, see below) are shown in Figure 1. We focus here on the analysis of surface ozone.

[20] In Figure 1, we present the accumulated concentration from each source of tropospheric ozone: from the stratosphere first and then from the soils, lightning, biomass burning, and anthropogenic NO_x source, respectively. In addition, the annual average bias (calculated as the average difference between model and observations) is indicated for each station.

[21] There is a slight positive model bias at the selected European continental sites. Clearly, over these regions, anthropogenic emissions are the main contributor to the surface ozone concentration. Similar relative contributions occur at the Tateno (Japan) station; in addition, at that location, during the summertime monsoon the model underestimates the ozone (this is not just a surface bias but occurs at all levels below 500 hPa; see Figure 2 discussed below), with a negative model bias in July and August of ~20 ppbv. Interestingly, this negative bias is also present in the work by *Lawrence et al.* [1999] and *Mickley et al.* [2001]. Over all the analyzed stations, the stratospheric contribution is rather small.

[22] The most important influences for Brazzaville, Natal and Ascension Island are from soils, biomass burning and lightning. The model has little bias over Ascension Island while it overestimates the biomass burning influence in January and February in Natal (none of the other contributions indicate much seasonal variation) and underestimates the surface ozone over Brazzaville. At these stations, lightning always contributes 3–5 ppbv of ozone at the surface.

[23] Finally, the ozone concentration at remote sites such as Aspendale is quite well captured, albeit with a somewhat reduced seasonal cycle and a slight underestimate during austral summer.

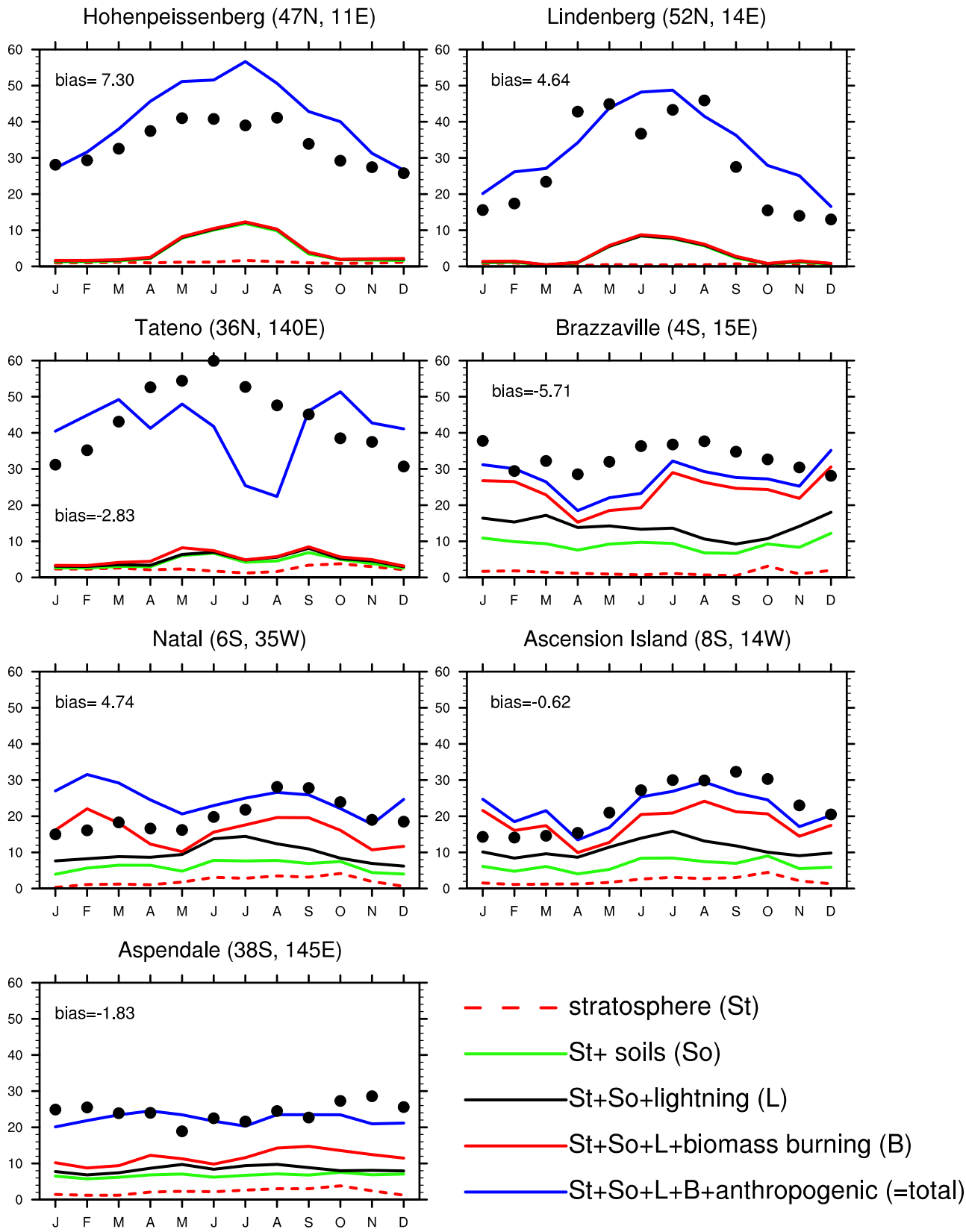

Figure 1. Monthly averaged surface ozone mixing ratio (in ppbv) for present-day conditions over selected sites for the model results and the observations from ozonesondes [*Logan*, 1999]. The line code represents the accumulated concentration from a variety of ozone sources, starting with stratospheric ozone; the observations are identified by the solid dots.

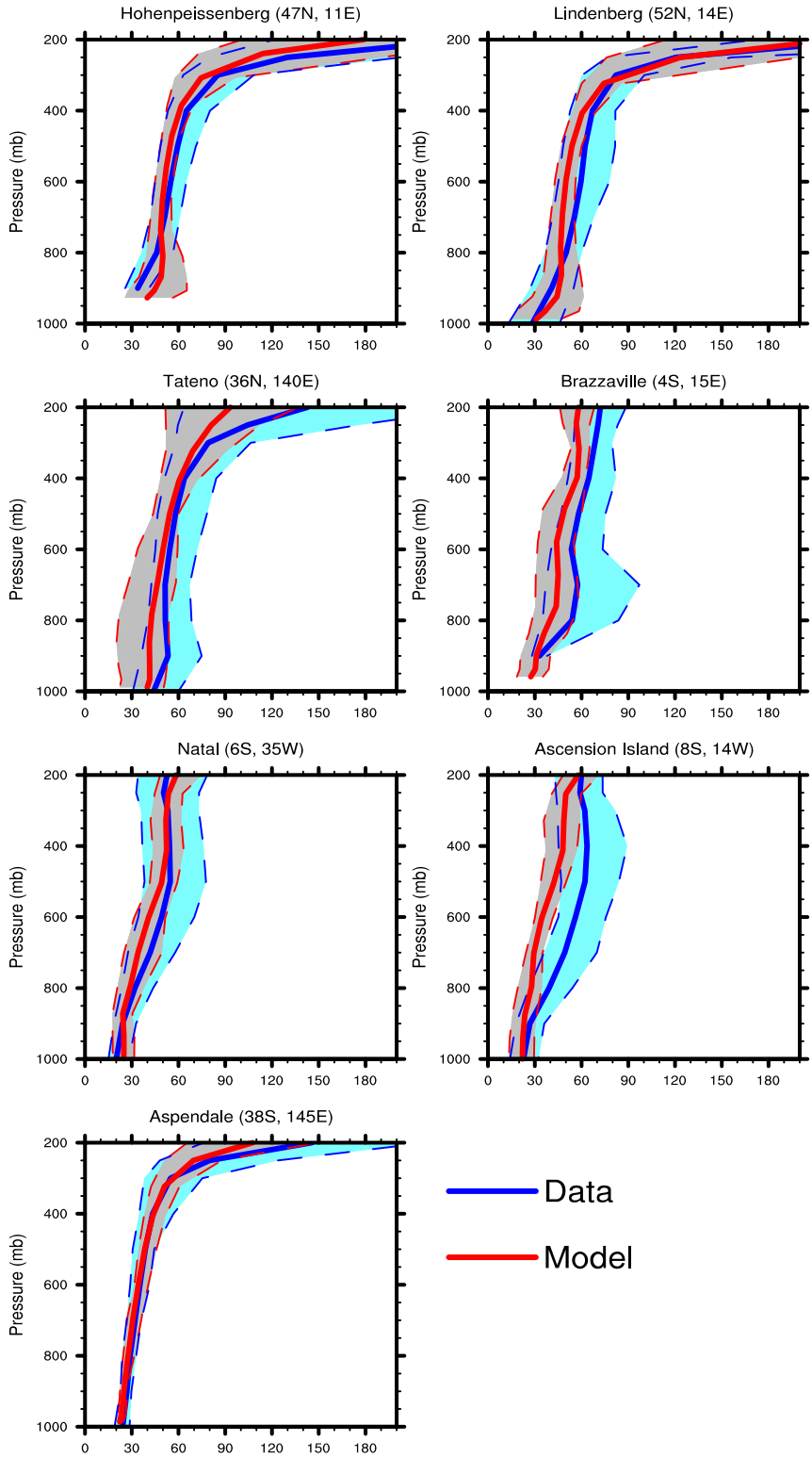

Figure 2. Annual average vertical profiles of ozone mixing ratio (in ppbv) for present-day conditions over selected sites for the model results and the observations [*Logan*, 1999]. The shaded areas (grey for model, blue for observations) indicate the range (minimum to maximum) of monthly values.

[24] Using the same stations, the comparison of mean ozone vertical profiles to observations indicates a good representation of the observed distribution, but with a tendency for a negative bias (Figure 2). This negative bias is more pronounced in the tropical regions, especially over Ascension Island. Also the model tends to have a reduced annual cycle (shown here by the envelope defined by the yearly minimum and maximum ozone concentrations) com-

pared to the observations. However, the upper troposphere to lower stratosphere transition in the midlatitudes region, a key region for the radiative forcing calculation, seems to be well captured by the model. Using all the stations from *Logan* [1999] with a long record (18 stations), we have found an average root-mean-square annual error of 20 ppbv (ranging between 4 and 50 ppbv) at 200 hPa.

4.2. Comparison With Turn-of-the-Century Observations

[25] There is a wealth of ozone observations in the late 19th and early 20th century [*Linvill et al.*, 1980; *Bojkov*, 1986; *Volz and Kley*, 1988; *Lisac and Grubišić*, 1991; *Cartalis and Varotsos*, 1994; *Marenco et al.*, 1994; *Pavelin et al.*, 1999]. Except for the Montsouris record [*Volz and Kley*, 1988], these observations are based on the Schönbein method. The Schönbein index is a very nonlinear function of ozone concentration and relative humidity [*Linvill et al.*, 1980]. Once the correction for relative humidity is applied, the conversion from the recorded color index of the Schönbein method to ozone concentration relies on the Montsouris measurements for which concurrent "direct" and Schönbein observations were made [*Bojkov*, 1986; *Marenco et al.*, 1994]. This procedure leads to surface ozone concentrations of 10 ppbv or less over most sites [*Hauglustaine and Brasseur*, 2001]. We will base our comparison on a subset of the compilation from *Hauglustaine and Brasseur* [2001].

[26] Regarding the Montsouris record, note that the 1876–1883 period used by *Hauglustaine and Brasseur* [2001] is actually the lowest ozone recorded for that station [see *Volz and Kley*, 1988, Figure 3]; in particular, the consideration of the measurements around the turn of the century would already increase the ozone concentration to ~15 ppbv (from less than 10 ppbv). In addition, it is important to remember that fairly large error bars (on the order of 25% [*Marenco et al.*, 1994]) should be added to the mean values. In particular, even the "direct" measurement technique in Montsouris suffers from SO_2 contamination, which *Volz and Kley* [1988] tried to minimize by filtering the original data.

[27] Over the next three subsections, we will discuss various aspects of our 1890 simulation results and the corresponding available ozone observations. The main points we want to highlight are that (1) it is not possible for our model to reproduce the Montsouris record, even with only natural NO_x sources; (2) whereas the anthropogenic emissions are not needed over Montsouris for the model to reproduce the observations, some seem to be required over Vienna; and (3) measurements at tropical sites such as Luanda and Rio de Janeiro are so low that the simulated ozone from natural sources alone already exceeds the measurements.

4.2.1. Analysis of the Modeled 1890 Surface Ozone

[28] Analysis of our 1890 (Figure 3) simulation indicates surface values with a positive mean model bias (model minus observations). Except for a few locations (Adelaide and Cordoba), this positive bias is of the order 5 to 25 ppbv. Note that the modeled Tokyo summertime concentrations suffer from the same negative bias as the present-day simulation (Figure 1). The overall positive bias found in this study is similar to the studies by *Wang and Jacob* [1998], *Mickley et al.* [1999] and *Shindell et al.* [2003], but considerably larger than *Berntsen et al.* [1997] or *Hauglustaine and Brasseur* [2001]. However, the global ozone deposition flux in these last two papers seems to be much larger than our estimates (see section 7). We discuss this point in more detail in section 4.3.2.

[29] In our simulation of the Montsouris record, the largest contributor by far is the anthropogenic emissions. However, in Montsouris, the recorded levels are so low that the sum of the stratospheric source and the ozone associated with soil and lightning NO_x emissions alone would be very similar to the observations. In addition it is possible that the stratospheric contribution to surface ozone could be larger than estimated here; indeed STE fluxes of ozone are usually considered to be around 500 Tg for present-day conditions [*Olsen et al.*, 2002] and stratospheric ozone was most likely larger in preindustrial times [*Staehelin et al.*, 1998; *Shindell and Faluvegi*, 2003].

[30] The large simulated anthropogenic ozone contribution over Montsouris could be seen as the reason for the high bias against observations. However, the same anthropogenic emissions scenario creates a smaller bias when compared to the Vienna record. Under the assumption that the observations from these two sites are quantitatively useful or at least suffer from the same biases, this indicates an inconsistency in the importance of anthropogenic emissions over Europe in 1890.

4.2.2. Tropical Biomass Burning Estimates

[31] In the case of the South American stations, regions with similar emissions and chemical loss and production rates also lead to quite different biases when compared to observations. In particular, the measured Rio de Janeiro ozone record is at most times as small as the stratospheric contribution alone, while the Cordoba record requires the addition of at least the soils and lightning contribution. Finally, the measured ozone in Luanda is always smaller than the sum of the stratospheric and soils contribution. Even if biomass burning emissions were set to 1/10 of their present-day values (as in most other model studies of preindustrial ozone, see references in Table 2), this would still not lead to an agreement with the observations.

4.2.3. Ozone Observations in the First Half of the 20th Century Over Europe

[32] In most places, the use of the Schönbein method stopped in the first decades of the 20th century (some data are still available for the 1920s). While the number of total column ozone measurements (unfortunately not very useful for this study) rapidly increased from the use of Dobson spectrometers [*Dobson and Harrison*, 1926; *Craig*, 1950], surface measurements are scarce in the 1910–1950 period. The earliest measurements of surface ozone we found, measurements by absorption of ultraviolet light from artificial sources, were presented by *Dobson* [1936]. This paper lists surface measurements in Europe (France, Germany, and Switzerland) with an average concentration of 20 ppbv, consistent with the list of observations in the 1930s provided by *Staehelin et al.* [1994]. In addition, daily measurements from 29 December 1934 to 6 March 1935 in Abisko, Finland, indicate an average wintertime concentration of 19 ppbv [*Barbier et al.*, 1936]. Finally, measurements in the Alps between 1933 and 1940 are 20–22 ppbv [*Marenco et al.*, 1994]. Our 1930 simulation indicates surface ozone mixing ratio at these locations in the range of 23 to 25 ppbv

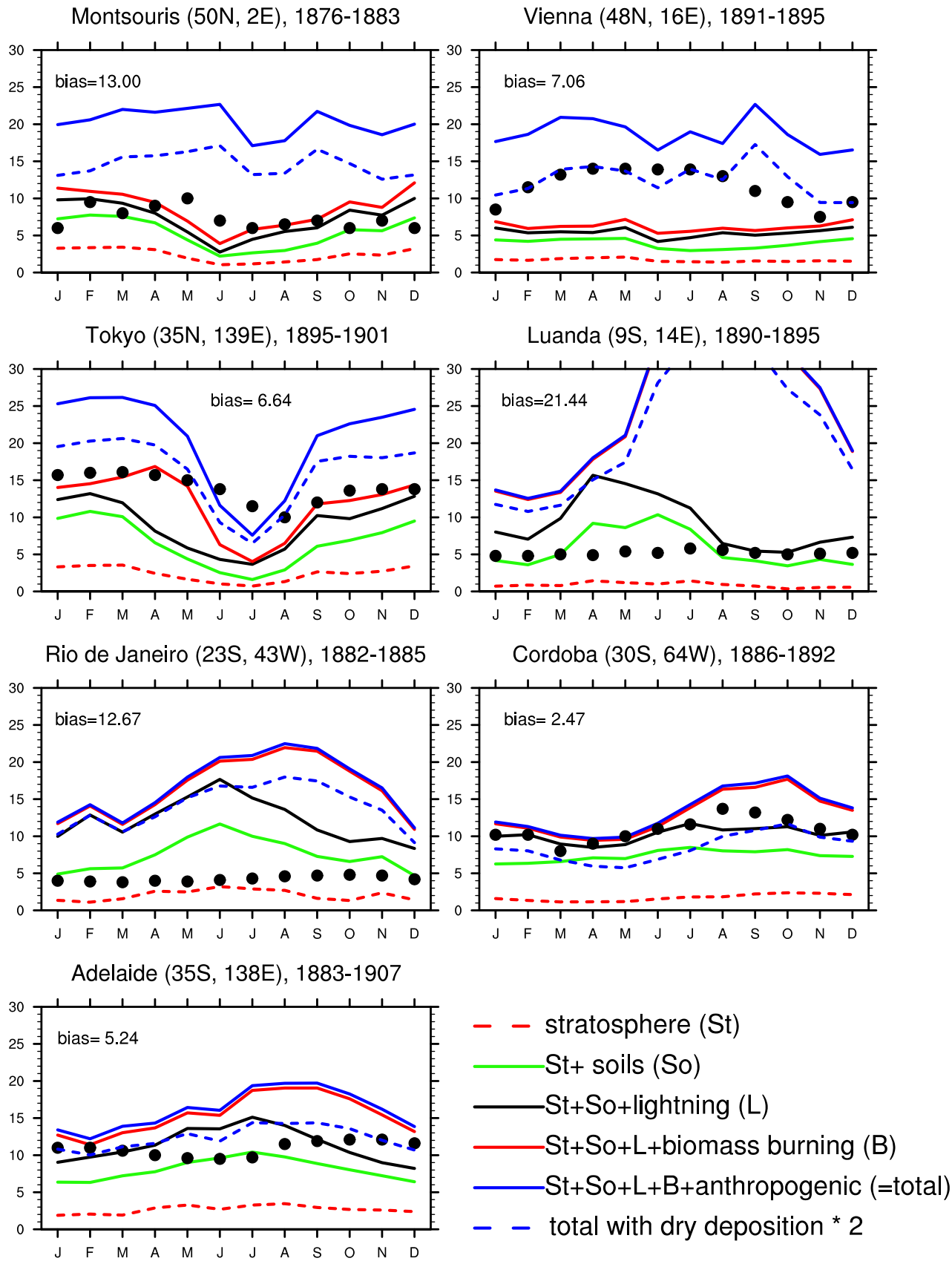

Figure 3. Monthly averaged surface ozone mixing ratio (in ppbv) for 1890 conditions over selected sites for the model results and the observations [*Hauglustaine and Brasseur*, 2001]. The line code represents the accumulated concentration from a variety of ozone sources, starting with stratospheric ozone; the observations are identified by the solid dots.

Table 2. Estimates of Tropospheric Ozone Increase From Preindustrial to Present From This Study and Other Previously Published Results

	Ozone Burden Increase, Tg
Berntsen et al. [1997]	102
Levy et al. [1997]	83
Roelofs et al. [1997]	81
Wang and Jacob [1998]	120
Mickley et al. [1999]	130
Lelieveld and Dentener [2000]	84
Hauglustaine and Brasseur [2001]	75
Shindell et al. [2003]	94
Wong et al. [2004]	140
This study (all sources)	71
This study (no 1890 anthropogenic source)	88

(remember that, as seen in Figure 3, the seasonal cycle over European stations is quite limited). This points toward a possible 3–5 ppbv bias in our model results, quite reduced from the one found in the 1890 analysis for European stations. However, according to our model results, the ozone surface concentrations over many of the observational sites have changed little between 1890 and 1930 (see section 5). This circumstantial evidence further reinforces our belief that the Schönbein-based ozone records over Western Europe may be biased low for the period around the turn of the 20th century and are clearly very uncertain [*Pavelin et al.*, 1999].

4.3. Sensitivity Experiments

[33] In the next 2 subsections, we discuss results from some sensitivity simulations. These are aimed at comparing the sensitivity of our model results to previously published sensitivity experiments.

4.3.1. Modification of Natural Sources

[34] *Mickley et al.* [2001] aim to identify the best combination of preindustrial natural emissions that will match the observed record. In particular, they show that reducing soils and lightning NO_x emissions and increasing biogenic VOC emissions (to increase the ozone loss) helped match the observations. However, the same set of emission changes in a different model did not lead to the same level of improvements [*Shindell et al.*, 2003]. From our analysis, there is no consensus that the soils or lightning NO_x emissions need to be reduced globally; the modeled 1890 ozone distributions over Cordoba and Adelaide are well reproduced, while the same emissions lead to a large bias over Rio de Janeiro and to some extent Luanda. Reduction of the natural emissions as proposed by *Mickley et al.* [2001] would lead to a clear underestimate of the 1890 ozone surface concentration in Cordoba, Adelaide and Luanda (not shown).

4.3.2. Sensitivity to Dry Deposition

[35] To test the importance of ozone dry deposition, we have performed a sensitivity test in which the deposition velocity was doubled (see dashed blue line in Figure 3). Over Montsouris and Vienna, this has the consequence of decreasing the simulated mixing ratio by 5–7 ppbv, although not enough to eliminate the bias for Montsouris. However, we have no reason to believe that our ozone dry deposition velocity (based on the Wesely scheme [*Wesely*, 1989; *Walmsley and Wesely*, 1996; *Wesely and Hicks*, 2000]) is wrong by a factor of 2. In particular, comparison of observed ozone deposition at Harvard Forest with our model results indicates a difference in the long-term average smaller than 20% (E. Davin, personal communication, 2003). Furthermore, our large-scale distribution of ozone deposition velocities is very similar to the independent model of *Ganzeveld and Lelieveld* [1995]. Consequently, while the ozone deposition velocity clearly plays a role, it cannot be the main source of the positive bias in our model. The contribution of dry deposition to the tropospheric ozone budget in this model is further discussed in section 7.

5. Regional Distribution of Ozone Changes From 1890

[36] We present here the changes in the annual distribution of surface ozone since 1890. For that purpose, we display in Figure 4 the difference in the ozone surface concentration between the considered simulation (1910 through 1990) and 1890. Because of some interannual variability, this difference can lead to local negative values, even though the emission of ozone precursors (and the global ozone burden, see section 7) have steadily increased during the 20th century.

[37] In 1910, most of the changes are limited to the industrial zones of Europe and North America. Some biomass burning associated with tropical deforestation is also taking place and is indicated by the ozone increase over South America. By 1930, there is a clear demarcation between the northern extratropics and the rest of the world, indicating the more rapid and widespread increase of ozone north of the Equator. By 1950 the presence of the Californian sources is much more noticeable, as is the location of the maximum European pollution over the Mediterranean Sea. After 1950, there is a rapid increase in the surface ozone concentration, with the whole region north of 30°N characterized by an increase larger than 10 ppbv over the 1890 distribution. This rapid increase was also noted in the analysis of trends in the observational record [*Staehelin et al.*, 1994, 1998]. Finally, the distribution in 1990 is specific in its impact of industrialization over the Southeast Asian and Indian regions. Similarly, most of the Southern Hemisphere land areas are at this point affected by large localized sources around 30°S, in addition to a hemispheric increase of ~5 ppbv above the 1890 levels by 1970. When the 1890 anthropogenic emissions are set to 0, then the increase of ozone over most of the Northern Hemisphere is significantly larger (see right bottom panel of Figure 4). This increase is more directly comparable to previously published analyses of the preindustrial to present ozone increase.

6. Contrasting 1890 and 1990 Sources of Ozone

[38] We use the tagging of tropospheric and stratospheric ozone to identify the main contributors to the large-scale ozone distribution. While it is clear that anthropogenic emissions are responsible for the ozone increase in developed regions (such as Europe and North America), it is interesting to expand the analysis to the globe. We will focus our analysis on the surface ozone concentration.

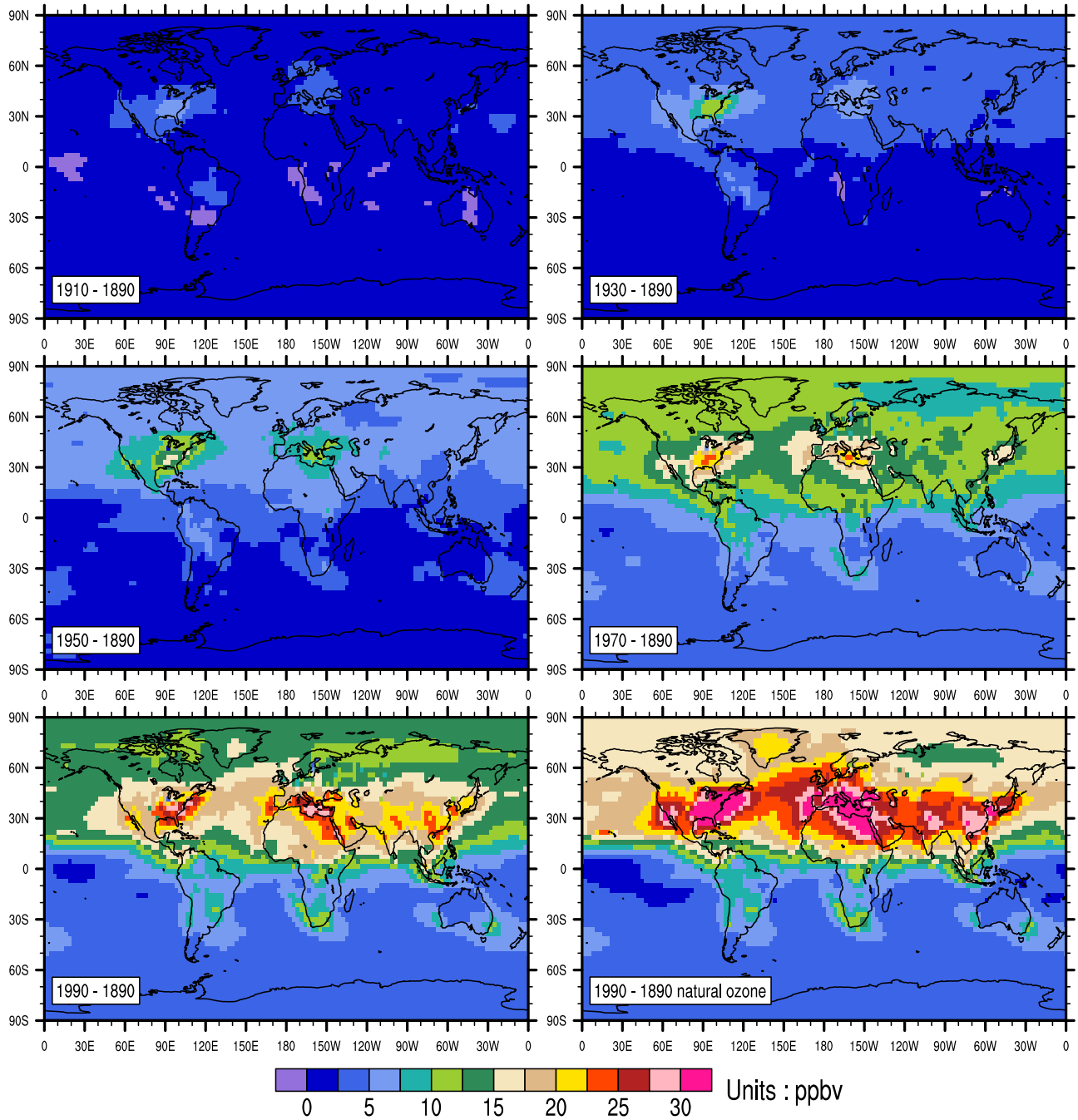

Figure 4. Annual average of the surface ozone increase (in ppbv) from the 1890 distribution. The right bottom panel is the surface ozone increase (in ppbv) from the 1890 ozone distribution obtained without anthropogenic emissions.

[39] The annual average relative contribution (in %) of the anthropogenic, natural (associated with soil, biomass burning and lightning NO_x emissions) and stratospheric source of ozone are shown in Figure 5 for the 1890 and 1990 simulations.

[40] On an annual average, the importance of stratospheric ozone is never larger than 30%, even in the most pristine environment of the Southern Hemisphere in 1890. Our estimate of the stratospheric portion of the surface ozone is smaller than other studies (e.g., *Wang and Jacob* [1998] or *Hauglustaine and Brasseur* [2001]). This is most likely due to differences in the definition of the stratospheric portion of tropospheric ozone. In addition, the decrease of the stratospheric fraction in surface ozone between 1890 and 1990 is due to the overall increase of surface ozone combined.

[41] The role of natural emissions has obviously decreased significantly over most of the Northern Hemisphere. At most, the contribution from the natural sources of NO_x is of the order of 30% in 1990.

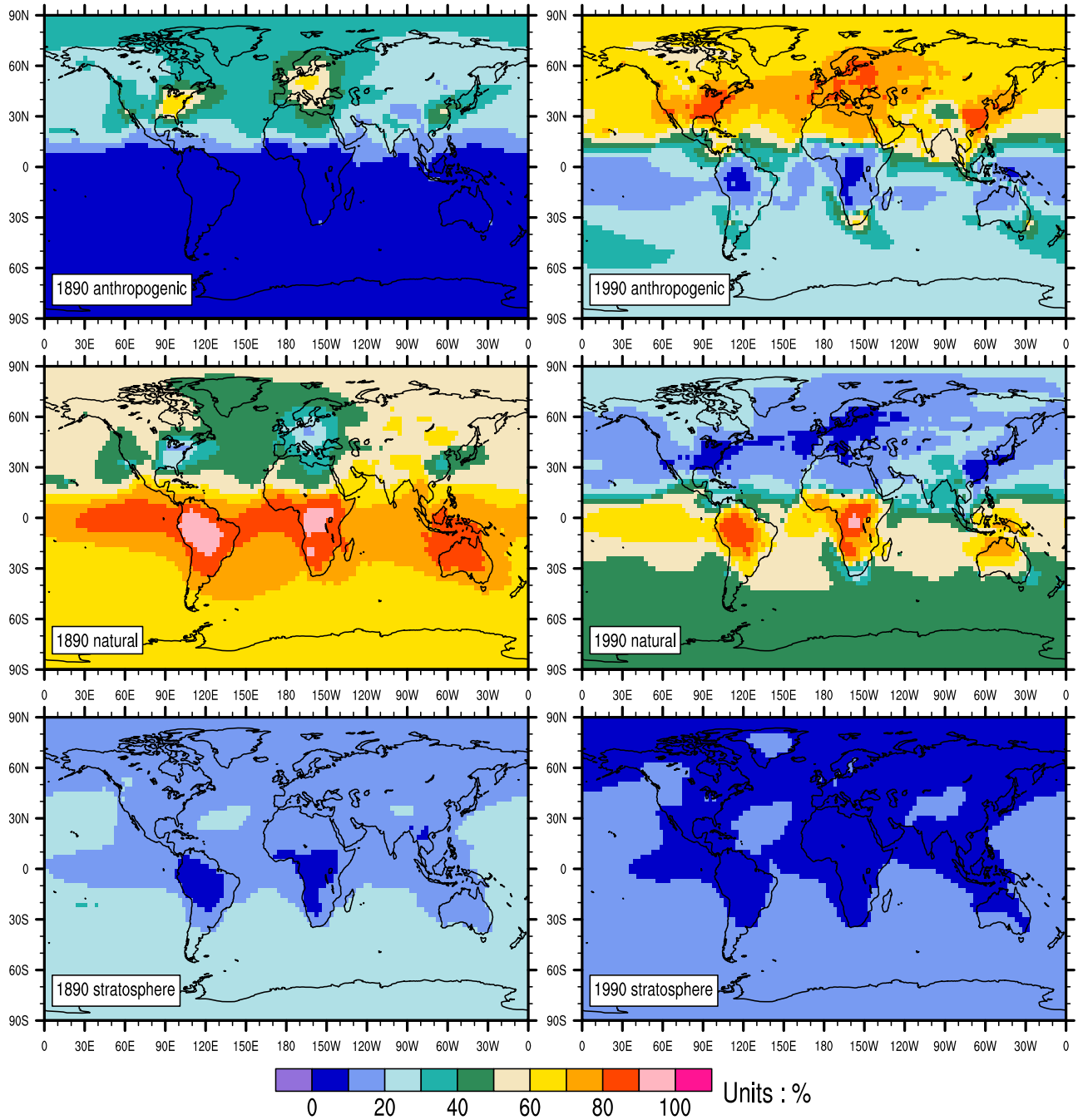

Figure 5. Contribution to the surface ozone mixing ratio (in %) from (top) anthropogenic, (middle) natural, and (bottom) stratospheric sources of ozone in (left) 1890 and (right) 1990.

[42] Next, we look at the relative contribution of each natural source of NO_x (biomass burning, lightning and soils) to the combined natural ozone concentration. Within these natural sources of NO_x, the relative role of soils to the ozone budget over the northern midlatitudes has considerably increased from the use of fertilizers (Figure 6). While the use of fertilizers in Africa is not as abundant as in the Northern Hemisphere, it has a significant impact on the role of soil emissions on the ozone concentration over this region, where in 1990 less than 20% of the simulated ozone is of anthropogenic origin (Figure 5). Over the tropical Pacific Ocean, the relative role of lightning is virtually unchanged between 1890 and 1990. Downstream from fertilized regions, the contribution of lightning to the natural source of ozone has decreased by 10–20%.

7. Ozone Budget in the 20th Century

[43] For each of the 20-year time samples between 1890 and 1990, we have computed the following tropospheric ozone global budget terms: chemical production, chemical loss, net chemical production, surface deposition and burden. In this study we compute the budget on the model levels from the surface up to 200 hPa. In addition, we have

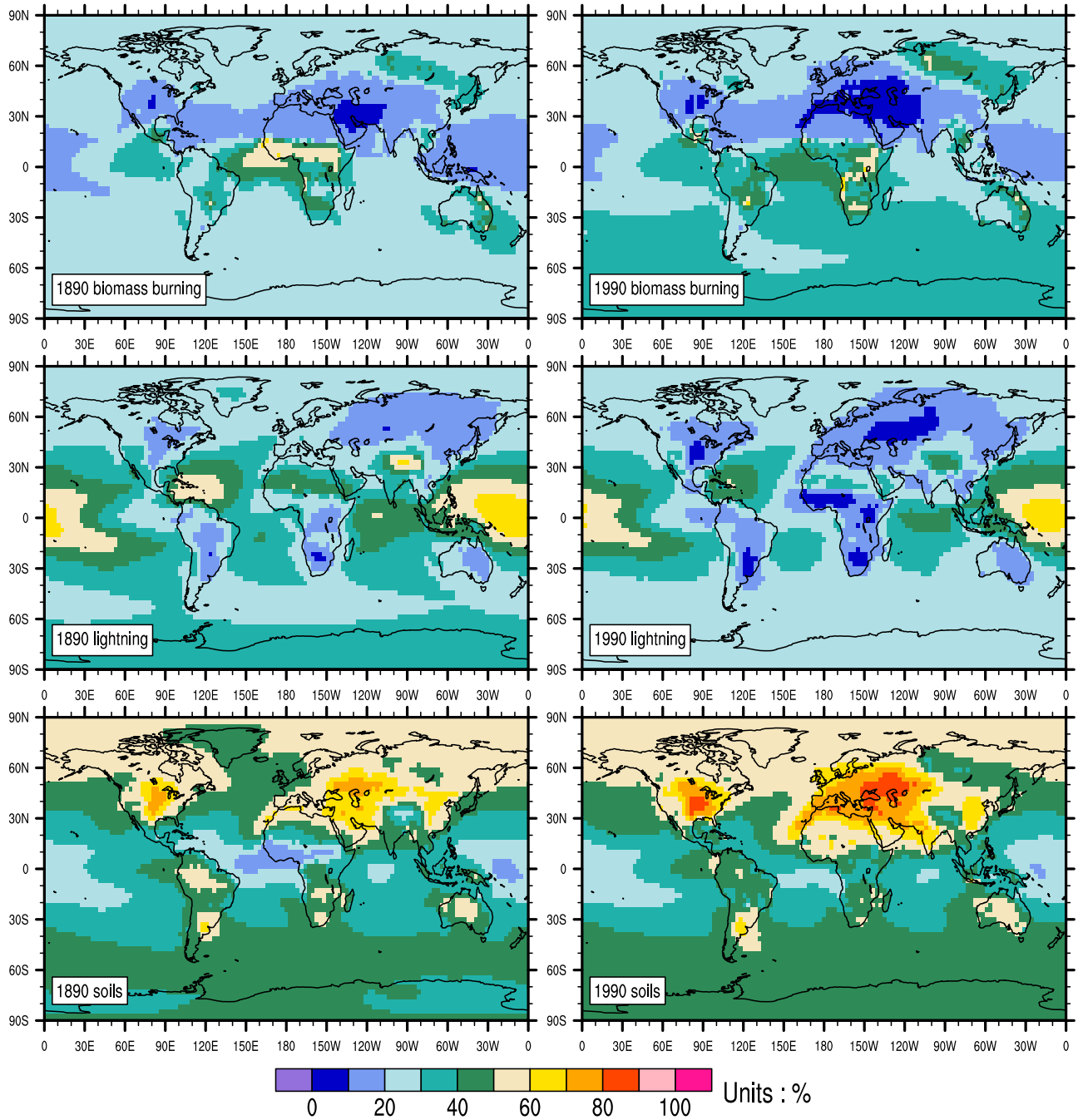

Figure 6. Contribution to the surface ozone mixing ratio of natural origin (in %) from (top) biomass burning, (middle) lightning, and (bottom) soils NO_x sources in (left) 1890 and (right) 1990.

computed the budget terms separately in the lower troposphere (pressure greater than 800 hPa) and free troposphere (above 800 hPa and below 200 hPa). The flux of stratosphere-troposphere exchange is ~400 Tg/yr and therefore not discussed.

[44] Between 1890 and 1990, the tropospheric ozone burden simulated in this study increases from 203 Tg to 274 Tg (Figure 7), an increase of 71 Tg. This estimate is on the low side of other published estimates (see Table 2). However, all these other studies have no preindustrial anthropogenic emissions and biomass burning emissions set to 10% (20% in the study by *Stevenson et al.* [1998]) of the present-day values, except for the study by *Lelieved and Dentener* [2000], who used emission scenarios similar to our study but focused on 1860. In our study the consideration of some anthropogenic emissions in 1890 creates a tropospheric ozone burden that is ~17 Tg; therefore the more meaningful tropospheric ozone burden increase to compare to other studies is 88 Tg, slightly below the average of the estimates in Table 2. In addition, our using biomass preindustrial biomass burning emissions that are larger than most the other studies also leads to a smaller increase in tropospheric ozone burden between 1890 and 1990; indeed, as shown by *Wang and Jacob* [1998], the

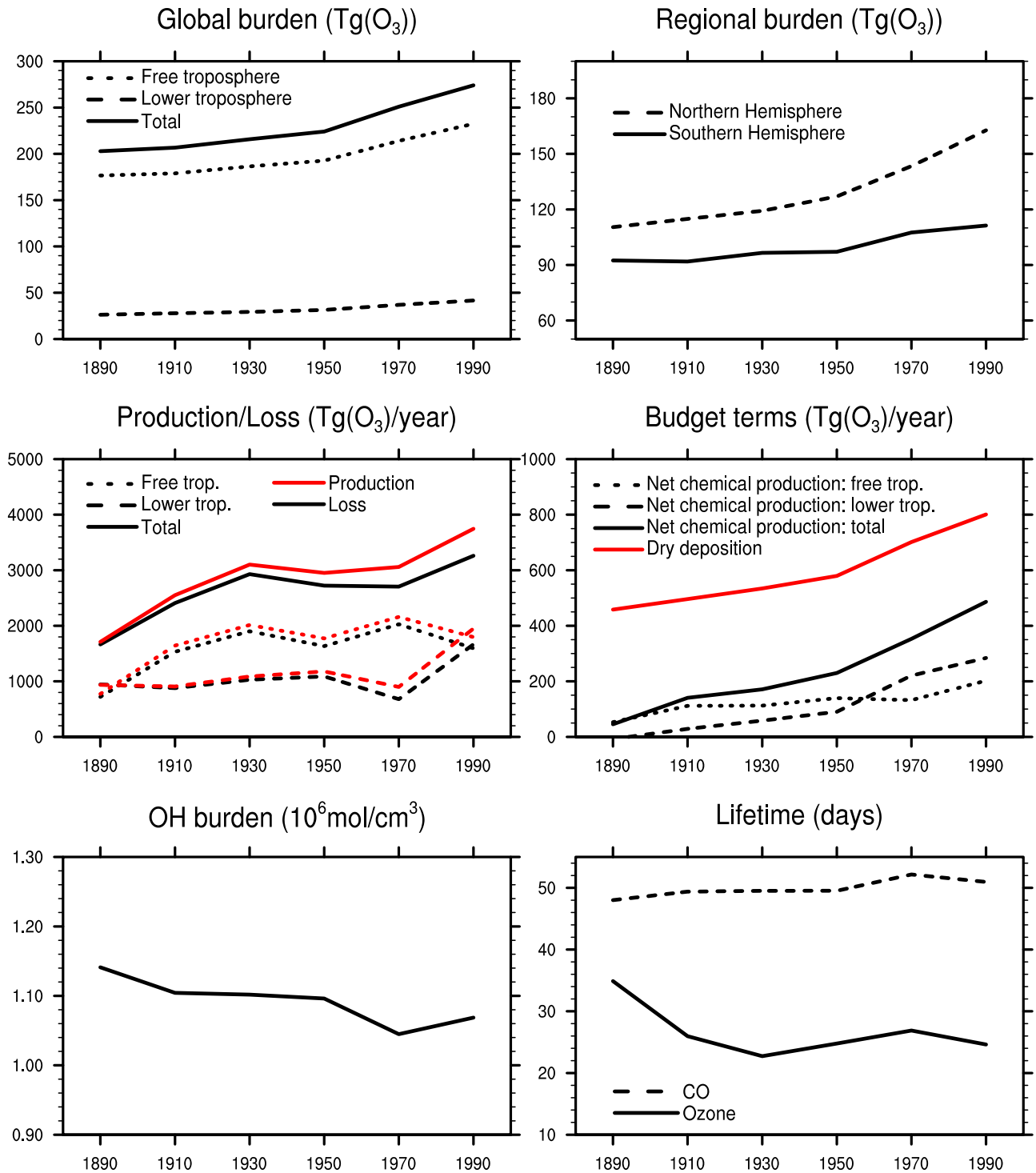

Figure 7. Time evolution of various integrated quantities of the tropospheric ozone budget. The integrals are taken over the globe and from the surface up to 200 hPa.

consideration of present-day biomass burning in preindustrial simulations lowered their estimated tropospheric ozone increase from 120 Tg to 87 Tg.

[45] Between 1890 and 1990, the free troposphere sees an increase in the tropospheric ozone burden of 56 Tg (from 176 Tg to 232 Tg, or an increase of 32% over the 1890 burden). In the lower troposphere, the increase is even more pronounced, from 26 Tg to 41 Tg, an increase of 58%.

[46] In the course of this study, we also performed experiments in which the stratosphere-troposphere exchange (STE) was left unconstrained. This led to ozone fluxes (~700 Tg) significantly larger than the 400 Tg used in SYNOZ. Because of the 25-day ozone lifetime, this large increase is only weakly reflected by an increased tropospheric ozone burden of ~30 Tg, similar to our findings in a very different model framework [*Lamarque et al.*, 1999]. In addition, as

there is no a priori reason to think that the ozone STE flux has substantially changed between 1890 and 1990 (it might actually have decreased slightly due to the CFC-induced stratospheric ozone depletion), we believe the tropospheric ozone burden increase is not very sensitive to the actual value of the STE flux, as long as it is reasonable.

[47] The increase in tropospheric ozone burden occurs in both hemispheres. In the Northern Hemisphere, this increase was particularly rapid after 1950, similar to the conclusions of *Staehelin et al.* [1994]. However, in the Southern Hemisphere, the increase is significant only after 1970. Overall, the Northern Hemisphere is characterized by an almost exponential growth in tropospheric burden, as could be expected from increased NO_x emissions (Table 1).

[48] Over the 1890–1990 period, the chemical production of ozone has increased more rapidly than its chemical loss. The growth in the chemical production and loss was rapid between 1890 and 1930, then flat until another rise after 1970. Until 1970, the growth in the chemical tendencies is limited to the free troposphere.

[49] The tropospheric ozone burden increase is directly related to the increased net chemical production, from 45 to 486 Tg/yr. This increase has been much more rapid in the lower troposphere, especially after 1950, when the net production in the lower troposphere is for the first time larger than in the free troposphere. In response to an increased tropospheric burden, the deposition flux has almost doubled, from 460 to 800 Tg/yr. As mentioned in section 4, our deposition flux is considerably (by at least 30%) smaller than *Berntsen et al.* [1997], *Hauglustaine and Brasseur* [2001], or *Wong et al.* [2004]. It is, however, in good agreement with the overall range of present-day model studies of *Prather et al.* [2001].

[50] The ozone lifetime (calculated as the burden divided by the photochemical and dry deposition loss [*Horowitz et al.*, 2003]) changes from 35 days in 1890 to 25 days in 1990. It is interesting to note that in our study, the ozone lifetime decreases rapidly between 1890 and 1930 and stays fairly constant after that. The overall decrease between 1890 and 1990 is more pronounced than by *Wang and Jacob* [1998] or *Hauglustaine and Brasseur* [2001] but in agreement with *Stevenson et al.* [1998] and *Mickley et al.* [1999]. Since the ozone lifetime varies strongly with latitude and altitude, the changes in the ozone lifetime are also a reflection of the changes in its distribution.

[51] The mass-weighted mean tropospheric OH (approximately 1.1×10^6 molecules/cm^3 in 1990, in agreement with the range of *Lawrence et al.* [2001] and *Prinn et al.* [2001]) is shown to decrease by ~8%. Other model studies have shown a decrease by 9% [*Wang and Jacob*, 1998], 16% [*Mickley et al.*, 1999], 17% [*Brasseur et al.*, 1998] and 33% [*Hauglustaine and Brasseur*, 2001] or a 7% increase [*Berntsen et al.*, 1997]. The overall decrease is most likely very dependent on the meteorological fields used to drive the model, and specifically on the amount of tropospheric water vapor. As a consequence of the OH trend, the carbon monoxide (CO) lifetime has increased from 47 to 51 days. It is unclear why the 1970 simulation exhibits a somewhat discontinuous pattern in the OH amount. It is, however, interesting to note a similar positive OH trend between 1978 and 1990 shown by *Prinn et al.* [2001].

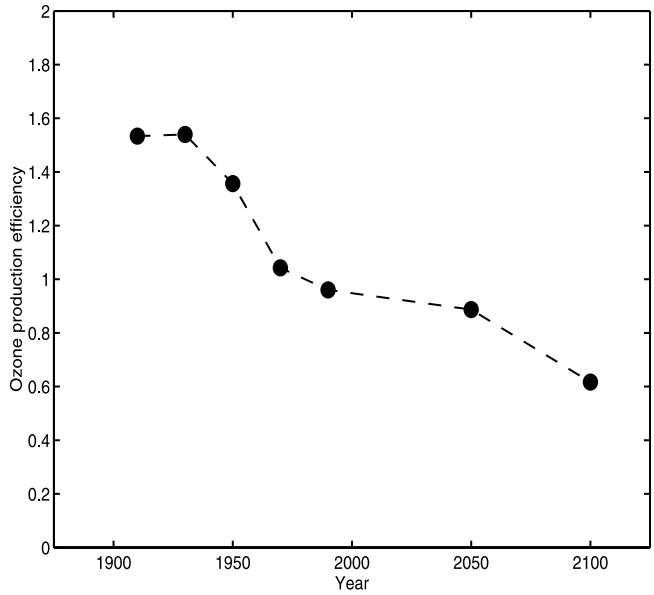

Figure 8. Time evolution of the ozone production efficiency, as calculated by the ratio of increased tropospheric burden to increase NO_x emissions from their 1890 values. The 2050 and 2100 NO_x emissions are from the SRES A2p scenario from *Prather et al.* [2001].

[52] To further investigate the relationship between emissions of ozone precursors and the tropospheric ozone burden, we present in Figure 8 the ratio of the globally averaged ozone burden increase (up to 400 hPa to limit the stratospheric influence) to the globally averaged NO_x emissions increase

$$\frac{O_3(\text{year}) - O_3(1890)}{NO_x(\text{year}) - NO_x(1890)}$$

where O_3 and NO_x are expressed in Tg. Figure 8 illustrates the ability of the troposphere to process the larger and larger emissions of ozone precursors released at the surface. In addition to the simulations discussed in this paper, we have included results from similar simulations but in which the 2050 and 2100 emissions are taken from the Special Report on Emissions Scenarios [*Nakicenovic et al.*, 2000] (SRES) A2p scenario [*Prather et al.*, 2001], usually considered the worst-case scenario with a very large increase in NO_x emissions and other ozone precursors. During the 20th century, the ozone production efficiency associated with the NO_x emissions decreases, similar to the findings of *Liu et al.* [1987] and *Wang and Jacob* [1998]. Under the assumed A2p scenario, this decrease (of ~50%) continues during the 21st century. In addition, after a relatively stable ratio from 1970 to 2050, the 2100 simulation exhibits a significant drop in the ozone production relative to the NO_x emissions. The reason for this behavior is being investigated.

[53] The overall decrease in ozone production efficiency implies that, under the assumed increase in NO_x emissions in the A2p scenario, there will be less NO_x limitation in the troposphere during the 21st century. This also indicates that the use of a single parameter relating increase tropospheric

ozone burden to NO_x emissions (e.g., as used in Table 4.11 of *Prather et al.* [2001]) is a rather crude approximation.

8. Discussion and Conclusions

[54] In this study, we have simulated the evolution of tropospheric ozone between 1890 and 1990 at 20-year intervals using estimated ozone precursors emissions based on the EDGAR-HYDE emission estimates [*van Aardenne et al.*, 2001] and meteorological fields from *Washington et al.* [2000]. The comparison with present-day observations indicates a very good overall performance of the model; on the other hand, our 1890 simulation overestimates the measured ozone, especially over Montsouris. In particular, it is not possible for our model to reproduce the Montsouris record, even when considering only the natural sources of NO_x; in addition, measurements at tropical sites such as Luanda and Rio de Janeiro are so low that the simulated ozone from natural sources alone exceeds the measurements. Overall, these results suggest that the ozone proxy measurements from the end of the 19th century have to be used very cautiously.

[55] The simulations performed in this study include some anthropogenic emissions in 1890, as can be expected from the existence of industries and large population centers in the Northern Hemisphere. The separate impact of these emissions on the ozone budget was shown to be responsible for ~8% (17 Tg out of 203 Tg) of the tropospheric ozone burden in 1890. Using the emissions from *van Aardenne et al.* [2001], our simulations show a tropospheric ozone burden increase of 71 Tg between 1890 and 1990. When the contribution to the ozone burden from anthropongenic emissions are removed (for direct comparison with the preindustrial studies), our estimate of the simulated increased tropospheric ozone burden between 1890 and 1990 (88 Tg) is in good agreement with previously published estimates.

[56] The ozone burden is shown to have more rapidly increased in the lower troposphere (at pressures higher than 800 hPa) than in the free troposphere; in particular, the net ozone production in the lower troposphere surpasses the net ozone production in the free troposphere between 1950 and 1970. In addition, we showed that the ozone production in this study increased rapidly between 1890 and 1930 and from 1970 to 1990 (the last simulated period). During all periods, the ozone chemical production has risen faster than its chemical destruction. In addition, the ozone lifetime has decreased from 35 days in 1890 to 25 days in 1990.

[57] The tropospheric ozone increase has been largest in the Northern Hemisphere, following its rapid industrialization. However, the ozone production efficiency associated with NO_x emissions has been decreasing from 1890, especially after 1930. The overall evolution of the tropospheric chemistry system is toward being less and less NO_x-limited overall. Using the A2p scenario, we have shown that this negative trend is likely to continue into the 21st century.

[58] In conjunction with increased tropospheric methane concentrations, the OH burden is shown to have decreased by ~8% between 1890 and 1990, with a concurrent increase in the CO lifetime.

[59] The importance of chemistry in shaping the lifetime of greenhouse gases and aerosols will need to be investigated more, both for the recent past and the future, with the ultimate goal of incorporating and understanding the feedbacks between chemistry and climate.

[60] **Acknowledgments.** We would like to thank D. Kinnison and B. Ridley for their comments on a previous version of this manuscript. Three anonymous reviewers have provided very valuable input to improve this document. J.F.L. was supported by the SciDAC project from the Department of Energy. The National Center for Atmospheric Research is operated by the University Corporation for Atmospheric Research under sponsorship of the National Science Foundation.

References

Barbier, D., D. Chalonge, and É. Vassy (1936), Mesure de la teneur en ozone des couches basses de l'atmosphère pendant l'hiver, *C. R. Hebd. Séances Acad. Sci.*, *202*, 1525–1527.

Berntsen, T. K., I. S. A. Isaksen, G. Myhre, J. S. Fuglestvedt, F. Stordal, T. Alsvik Larsen, R. S. Freckleton, and K. P. Shine (1997), Effects of anthropogenic emissions on tropospheric ozone and its radiative forcing, *J. Geophys. Res.*, *102*, 28,101–28,126.

Bojkov, R. D. (1986), Surface ozone during the second half of the nineteenth century, *J. Clim. Appl. Meteorol.*, *25*, 343–352.

Brasseur, G. P., D. A. Hauglustaine, S. Walters, P. J. Rasch, J.-F. Müller, C. Granier, and X. X. Tie (1998), MOZART, a global chemical transport model for ozone and related chemical tracers: 1. Model description, *J. Geophys. Res.*, *103*, 28,265–28,289.

Campbell, I. D., and M. D. Flannigan (2000), Long-term perspectives on fire-climate-vegetation relationships in the North American boreal forest, in *Fire, Climate Change, and Carbon Cycling in the Boreal Forest*, edited by E. Kasischke and B. J. Stocks, pp. 151–165, Springer, New York.

Cartalis, C., and C. Varotsos (1994), Surface ozone in Athens, Greece, at the beginning and at the end of the twentieth century, *Atmos. Environ.*, *28*, 3–8.

Clark, J. S. (1988), Effect of climate change on fire regimes in northwestern Minnesota, *Nature*, *334*, 233–234.

Clark, J. S., and J. Robinson (1993), Paleoecology of fire, in *Fire in the Environment*, edited by P. Crutzen and J. G. Goldammer, pp. 193–214, John Wiley, Hoboken, N. J.

Craig, R. A. (1950), The observations and photochemistry of atmospheric ozone and their meteorological significance, *Meteorol. Monogr.*, vol. 1(2), 50 pp., Am. Meteorol. Soc., Boston, Mass.

Dobson, G. M. B. (1936), The vertical distribution of ozone in the atmosphere, *Q. J. R. Meteorol. Soc.*, *62*, 14–16.

Dobson, G. M. B., and D. N. Harrison (1926), Measurements of the amount of ozone in the Earth's atmosphere and its relation to other geophysical conditions, *Proc. R. Soc. London, Ser. A*, *110*, 660–693.

Emmons, L. K., et al. (2003), Budget of tropospheric ozone during TOPSE from two chemical transport models, *J. Geophys. Res.*, *108*(D8), 8372, doi:10.1029/2002JD002665.

Ganzeveld, L., and J. Lelieveld (1995), Dry deposition parameterization in a chemistry general circulation model and its influence on the distribution of reactive trace gases, *J. Geophys. Res.*, *100*, 20,999–21,012.

Gauss, M., et al. (2003), Radiative forcing in the 21st century due to ozone changes in the troposphere and the lower stratosphere, *J. Geophys. Res.*, *108*(D9), 4292, doi:10.1029/2002JD002624.

Guenther, A., et al. (1995), A global model of natural volatile organic compound emissions, *J. Geophys. Res.*, *100*, 8873–8892.

Hauglustaine, D. A., and G. P. Brasseur (2001), Evolution of tropospheric ozone under anthropogenic activities and associated radiative forcing of climate, *J. Geophys. Res.*, *106*, 32,337–32,360.

Holdsworth, G., K. Higuchi, G. A. Zielinski, P. A. Mayewski, M. Wahlen, B. Deck, P. Chylek, B. Johnson, and P. Damiano (1996), Historical biomass burning: Late 19th century pioneer agriculture revolution in Northern Hemisphere ice core data and its atmospheric interpretation, *J. Geophys. Res.*, *101*, 23,317–23,334.

Horowitz, L. W., et al. (2003), A global simulation of tropospheric ozone and related tracers: Description and evaluation of MOZART, version 2, *J. Geophys. Res.*, *108*(D24), 4784, doi:10.1029/2002JD002853.

Ito, A., and J. E. Penner (2004), Global estimates of biomass burning emissions based on satellite imagery for the year 2000, *J. Geophys. Res.*, *109*, D14S05, doi:10.1029/2003JD004423.

Kiehl, J. T., T. L. Schneider, R. W. Portmann, and S. Solomon (1999), Climate forcing due to tropospheric and stratospheric ozone, *J. Geophys. Res.*, *104*, 31,239–31,254.

Lacis, A. A., D. J. Wuebbles, and J. A. Logan (1990), Radiative forcing by changes in the vertical distribution of ozone, *J. Geophys. Res.*, *95*, 9971–9981.

Lamarque, J.-F., P. G. Hess, and X. X. Tie (1999), Three-dimensional model study of the influence of stratosphere-troposphere exchange and its distribution on tropospheric chemistry, *J. Geophys. Res.*, *104*, 26,363–26,372.

Lawrence, M. G., P. J. Crutzen, P. J. Rasch, B. E. Eaton, and N. M. Mahowald (1999), A model for studies of tropospheric photochemistry: Description, global distributions, and evaluation, *J. Geophys. Res.*, *104*, 26,245–26,277.

Lawrence, M. G., P. Jöckel, and R. von Kuhlmann (2001), What does the global mean OH concentration tell us?, *Atmos. Chem. Phys.*, *1*, 37–49.

Lelieveld, J., and F. J. Dentener (2000), What controls tropospheric ozone?, *J. Geophys. Res.*, *105*, 3531–3551.

Levy, H., II, P. S. Kasibhatla, W. J. Moxim, A. A. Klonecki, A. I. Hirsch, S. J. Oltmans, and W. L. Chameides (1997), The global impact of human activity on tropospheric ozone, *Geophys. Res. Lett.*, *24*, 791–794.

Linvill, D. E., W. J. Hooker, and B. Olson (1980), Ozone in Michigan's environment 1876–1880, *Mon. Weather Rev.*, *108*, 1883–1891.

Lisac, I., and V. Grubišić (1991), An analysis of surface ozone data measured at the end of the 19th century in Zagreb, Yugoslavia, *Atmos. Environ., Part A*, *25*, 481–486.

Liu, S. C., M. Trainer, F. C. Fehsenfeld, D. D. Parrish, E. J. Williams, D. W. Fahey, G. Hübler, and P. C. Murphy (1987), Ozone production in the rural troposphere and the implications for regional and global ozone distributions, *J. Geophys. Res.*, *92*, 4191–4207.

Logan, J. A. (1999), An analysis of ozonesonde data for the troposphere: Recommendations for testing 3-D models and development of a gridded climatology for tropospheric ozone, *J. Geophys. Res.*, *104*, 16,115–16,149.

Marenco, A., H. Gouget, P. Nédélec, and J.-P. Pagés (1994), Evidence of a long-term increase in tropospheric ozone from Pic du Midi data series: Consequences: Positive radiative forcing, *J. Geophys. Res.*, *99*, 16,617–16,632.

McLinden, C. A., S. C. Olsen, B. Hannegan, O. Wild, M. J. Prather, and J. Sundet (2000), Stratospheric ozone in 3-D models: A simple chemistry and the cross-tropopause flux, *J. Geophys. Res.*, *105*, 14,653–14,666.

Mickley, L. J., P. P. Murti, D. J. Jacob, and J. A. Logan (1999), Radiative forcing from tropospheric ozone calculated with a unified chemistry-climate model, *J. Geophys. Res.*, *104*, 30,153–30,172.

Mickley, L. J., D. J. Jacob, and D. Rind (2001), Uncertainty in preindustrial abundance of tropospheric ozone: Implications for radiative forcing calculations, *J. Geophys. Res.*, *106*, 3389–3399.

Nakicenovic, N., et al. (2000), *Emissions Scenarios*, 599 pp., Cambridge Univ. Press, New York.

Olsen, M. A., A. R. Douglass, and M. R. Schoeberl (2002), Estimating downward cross-tropopause ozone flux using column ozone and potential vorticity, *J. Geophys. Res.*, *107*(D22), 4636, doi:10.1029/2001JD002041.

Pavelin, E. G., C. E. Johnson, S. Rughooputh, and R. Toumi (1999), Evaluation of pre-industrial surface ozone measurements made using Schönbein's method, *Atmos. Environ.*, *33*, 919–929.

Prather, M. J., et al. (2001), Atmospheric chemistry and greenhouse gases, in *Climate Change 2001*, pp. 239–287, Cambridge Univ. Press, New York.

Price, C., J. Penner, and M. Prather (1997), NO_x from lightning: 1. Global distribution based on lightning physics, *J. Geophys. Res.*, *102*, 5929–5941.

Prinn, R. G., et al. (2001), Evidence for substantial variations of atmospheric hydroxyl radicals in the past two decades, *Science*, *292*, 1882–1888.

Ramaswamy, V., et al. (2001), Atmospheric radiative forcing of climate change, in *Climate Change 2001*, pp. 349–416, Cambridge Univ. Press, New York.

Roelofs, G.-J., J. Lelieveld, and R. van Dorland (1997), A three-dimensional chemistry/general circulation model simulation of anthropogenically derived ozone in the troposphere and its radiative climate forcing, *J. Geophys. Res.*, *102*, 23,389–23,401.

Savarino, J., and M. Legrand (1998), High northern latitude forest fires and vegetation emissions over the last millennium inferred from the chemistry of a central Greenland ice core, *J. Geophys. Res.*, *103*, 8267–8279.

Shindell, D. T., and G. Faluvegi (2003), An exploration of ozone changes and their radiative forcing prior to the chlorofluorocarbon era, *Atmos. Chem. Phys.*, *2*, 363–374.

Shindell, D. T., G. Faluvegi, and N. Bell (2003), Preindustrial-to-present-day radiative forcing by tropospheric ozone from improved simulations with the GISS chemistry-climate GCM, *Atmos. Chem. Phys. Discuss.*, *3*, 3939–3989.

Shine, K. P., and P. M. F. de Forster (1999), The effect of human activity on radiative forcing of climate change: A review of recent developments, *Global Planet. Change*, *20*, 205–225.

Staehelin, J., J. Thudium, R. Buehler, A. Volz-Thomas, and W. Graber (1994), Trends in surface ozone concentrations at Arosa (Switzerland), *Atmos. Environ.*, *28*, 75–87.

Staehelin, J., R. Kegel, and N. R. P. Harris (1998), Trend analysis in the homogenized total ozone series of Arosa (Switzerland), 1926–1996, *J. Geophys. Res.*, *103*, 8389–8399.

Staehelin, J., N. R. P. Harris, C. Appenzeller, and J. Eberhard (2001), Ozone trends: A review, *Rev. Geophys.*, *39*, 231–290.

Stevenson, D. S., C. E. Johnson, W. J. Collins, R. G. Derwent, K. P. Shine, and J. M. Edwards (1998), Evolution of tropospheric ozone radiative forcing, *Geophys. Res. Lett.*, *25*, 3819–3822.

Tansey, K., et al. (2004), Vegetation burning in the year 2000: Global burned area estimates from SPOT VEGETATION data, *J. Geophys. Res.*, *109*, D14S03, doi:10.1029/2003JD003598.

van Aardenne, J. A., F. J. Dentener, J. G. J. Olivier, C. G. M. Klein Goldewijk, and J. Lelieveld (2001), A $1^\circ \times 1^\circ$ resolution data set of historical anthropogenic trace gas emissions for the period 1890–1990, *Global Biogeochem. Cycles*, *15*, 909–928.

van der Werf, G. R., J. T. Randerson, G. J. Collatz, and L. Giglio (2003), Carbon emissions from fires in tropical and subtropical regimes, *Global Change Biol.*, *9*, 547–562.

Volz, A., and D. Kley (1988), Evaluation of the Montsouris series of ozone measurements made in the nineteenth century, *Nature*, *332*, 240–242.

Walmsley, J. L., and M. L. Wesely (1996), Modification of coded parameterizations of surface resistances to gaseous dry deposition, *Atmos. Environ.*, *30*, 1181–1188.

Wang, Y., and D. J. Jacob (1998), Anthropogenic forcing on tropospheric ozone and OH since preindustrial times, *J. Geophys. Res.*, *103*, 31,123–31,135.

Washington, W. M., et al. (2000), Parallel climate model (PCM) control and transient simulations, *Clim. Dyn.*, *16*, 755–774.

Wesely, M. L. (1989), Parameterization of surface resistances to gaseous dry deposition in regional-scale numerical models, *Atmos. Environ.*, *23*, 1293–1304.

Wesely, M. L., and B. B. Hicks (2000), A review of the current status of knowledge on dry deposition, *Atmos. Environ.*, *34*, 2261–2282.

Wong, S., W. Wang, I. S. A. Isaksen, T. K. Berntsen, and J. K. Sundet (2004), A global climate-chemistry model study of present-day tropospheric chemistry and radiative forcing from changes in tropospheric O3 since the preindustrial period, *J. Geophys. Res.*, *109*, D11309, doi:10.1029/2003JD003998.

L. Buja and W. Washington, Climate and Global Dynamics Division, NCAR, 1850 Table Mesa Drive, Boulder, CO 80305, USA.

L. Emmons, P. Hess, and J.-F. Lamarque, Atmospheric Chemistry Division, NCAR, 1850 Table Mesa Drive, Boulder, CO 80305, USA. (lamar@ucar.edu)

C. Granier, Aeronomy Laboratory R/E/AL8, CIRES NOAA, 325 Broadway, Boulder, CO 80303, USA.